Final Analysis of HART II Blade Deflection Measurement

Oliver Schneider, Berend G. van der Wall
Institut für Flugsystemtechnik
Deutsches Zentrum für Luft- und Raumfahrt e.V. (DLR)
Braunschweig, Germany

The wind tunnel test of HART II (Higher Harmonic Control Aeroacoustic Rotor Test), performed in October 2001 in the Large Low-Speed Facility (LLF) of the German-Dutch Wind-tunnel (DNW), is part of an international cooperative program by the German DLR, French ONERA, DNW, NASA Langley and the US Army Aeroflightdynamics Directorate (AFDD). The main objective of the program is the investigation of rotor wake and its influence on rotor blade-vortex interaction (BVI) noise with and without higher harmonic pitch control (HHC). For blade position and deflection measurements the Stereo Pattern Recognition (SPR) technique was used for the first time. This technique is based on a 3-dimensional reconstruction of visible marker locations by using stereo camera images. An evaluation of these images leads to the spatial position of markers which are attached to each of the four blades and to the bottom of the fuselage and thus to the blade motion parameters in flap, lead-lag and torsion. In [1] the different analysis methods and post-processing of SPR data are presented and the advantages, drawbacks and the potential of this technology are shown. The calculations were done with respect to the data set received first, where a calibration method based on six calibration markers was used. The results presented in this paper refer to newer raw data, which are based on an improved calibration method. The differences in results obtained by the different analysis methods and the final results for all four rotor blades of the deflection measurements of the HART II tests are described.

Introduction

Within the framework of the US/German MoU and the US/French MoA the partners of the HART program performed a HHC rotor test called HART II in 2001 in order to now focus on the rotor wake and its development within the entire rotor disk [2], [3]. This test was conducted within a three week test campaign in October 2001 in the LLF of the DNW. A total amount of 63000 3C-PIV data sets had been taken, 33600 SPR and BTD (blade tip deflection) data sets, 183 rotor and balance data sets, 642 noise measurements and 157 blade pressure data sets. In total roughly a terabyte (1TB = 1000GB) of raw data did exist after the test. Main emphasis was put on the baseline case of HART (6°descent) plus the flight path variation of it, and the two HHC cases with settings for minimum vibration and minimum noise radiation.

SPR and BTD measurement set-up

The SPR and BTD measurements required four cameras widely spaced on ground. One pair of cameras focused on the advancing side of the rotor disk, and the other one on the retreating side. With this method, the spatial position of markers attached to each of the four blades and to the bottom of the fuselage is determined optically. The SPR technique is based on a 3-dimensional reconstruction of visible marker locations by using stereo camera images. The accuracy of marker position recognition theoretically is about 0.4 mm in x-, y- and z-direction. A more detailed description of the method is presented in [4].

In addition, the common support was used for one camera focusing on the 90° azimuth position

of the blade, and a second tower was holding another camera for a view on the 135° position. These two cameras were focused only on the blade tip at the respective azimuth positions in order to independently measure the blade tip's vertical, horizontal and pitch position. This setup was called BTD (blade tip deflection measurement). At these azimuths, the results of BTD can directly be used as validation of the SPR results. The setup is schematically given in Fig. 1.

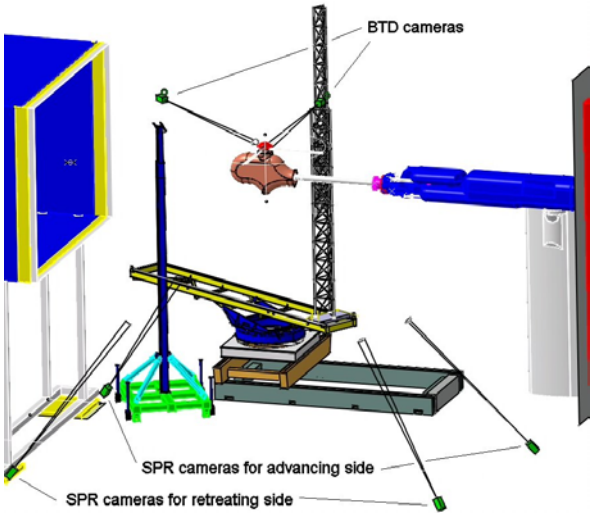

Fig. 1 Test setup for SPR and BTD measurements

The camera system was calibrated by using special calibration points. These were introduced by hanging 14 markers from the wind tunnel ceiling covering the whole rotor disk region at all possible measurement positions. The calibration measurements were done by using theodolites with an accuracy of 1 mm. By using a new improved least square calibration method 10 calibration markers plus 2 body marker locations (to extend the calibration volume over the complete body) were used (instead of 6 calibration markers as used for data in [1]) to calibrate each system of two SPR cameras (adv. / ret. side). This formed the basis of the mathematical model to recompute the blade marker positions in space from the two camera images in the aftermath and led to a completely new set of raw data which are used for all calculations described in this paper. More details about SPR were given in [4], the data acquisition system is described in [5].

Blade position measurements

For the HART II – test, a total of 36 markers (18 at the leading edge and 18 at the trailing edge, called blade marker, diameter 25 mm) were equipped on the lower side of each black painted rotor blade (see Fig. 2). Thus 18 radial stations were covered from r/R = 0.228 to 0.993. For purposes of hub center localization 4 markers were attached underneath the fuselage shell on a rectangular plate. These are called body markers herein.

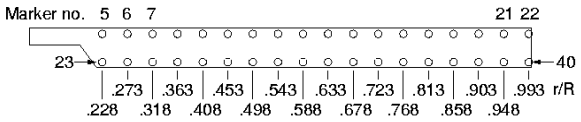

Fig. 2 Distribution of SPR markers on the rotor blades

The blade marker positions were measured optically by SPR technique with four floor-mounted cameras. A pair of them was focused on either half of the rotor disk such that the entire disk could be observed. The blade marker positions on the advancing side were measured by the upstream right and on the retreating side by the upstream left camera pair.

Data were taken at 15° azimuth increments totalling to 24 locations azimuthally such that the analysis allows synthesizing the lower harmonics from the time history of the blade motion over the entire length of the blade. SPR measurements were applied to the BL (base line configuration), MN (minimum noise configuration), MV (minimum vibration configuration) case, and to parts of the α-sweep, covering 6° and 3° climb and 12° descent (see Tab. 1).

Configuration	Shaft angle α_S	Comment
cal90	5.05° *	non-rotating calibration Ψ=90°
cal135	5.05° *	non-rotating calibration Ψ=135°
cal270	5.05° *	non-rotating calibration Ψ=270°
BL5.3	5.35°	Base line adv. side, 6° descent
BL5.3	5.265°	Base line ret. side, 6° descent
BL-3.7	-3.663°	Base line 3° climb
BL11.5	11.488°	Base line, 12° descent
MN5.3	5.315°	Minimum Noise, 6° descent
MV5.3	5.335°	Minimum Vibration, 6° descent
BL-6.9	-6.896°	Base line 6° climb

Tab. 1 Configurations of SPR measurements (* α_S=5.2° noted from DNW)

In total, 144 SPR measurements were made, wherein 24 contain 100 repeats (BL5.3) and the rest 50 repeats at the same location for statistical analysis. Since at each location all four blades are measured, this makes 33600 data sets of blade and body marker coordinates for post-processing. They stem from the same amount of camera raw data images.

An exemplary image of one SPR camera is given in Fig. 3. The blade is at a 90° azimuth position and the markers at leading and trailing edges as well as the body markers are clearly visible.

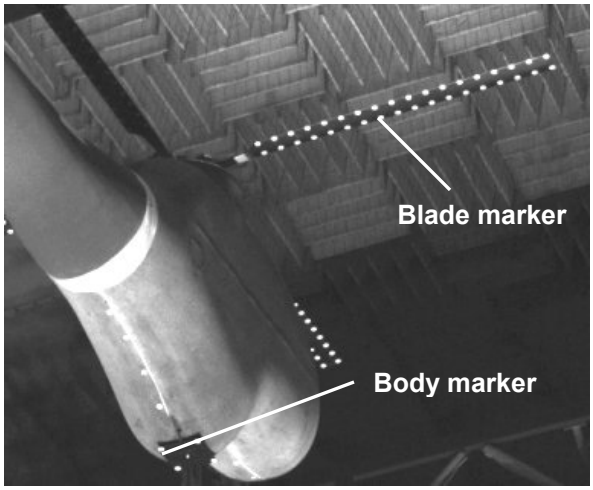

Fig. 3 SPR image of one camera at Ψ=90°

Evaluation of new SPR data

The analysis of SPR results requires some post-processing since the data contain only positions of the markers along leading and trailing edge in space, i.e. in the wind tunnel coordinate system. The goals are flap, lead-lag and torsion displacements of the quarter chord line in the shaft coordinate system with origin in the center of the rotor hub. To obtain these results, the position of the hub center must be known. The applied analyzing methods and their advantages and drawbacks are presented in [1].

Data in non-rotating system

After the new least error squares based SPR calibration method (with 10 calibration and 2 body markers) was evaluated new data from the non rotating system (Ψ=90° and Ψ=270°) were available. After rotation by the sting angle α_{Sting}=5.2° the blade marker z-positions depending on radius can be compared in the shaft axis system for Ψ=90° and Ψ=270°. Assuming similar blade material properties the quarter chord lines of these two azimuths should have the same radial z-deflection $z_{qc}(r)$, which was verified in laboratory tests.

Additionally to the new calibration a shifting of the images of the two front SPR-cameras by 2 pixels due to thermal expansion of the wind tunnel nozzle was identified and corrected. Furthermore, a third data point was available at Ψ=135°. By using the data point at Ψ=135° a determination of the correct shaft angle is possible by adapting the quarter chord lines of Ψ=90° and Ψ=135°. It means the quarter chord lines in a coordinate system parallel to the rotor shaft have the same deflection in z-direction if the wind tunnel coordinates are rotated by the correct shaft angle. In this kind a shaft angle of α_S=5.05° was determined. The difference to the sting angle 5.2° is due to support elasticity which was verified at other date during the test. The resulting quarter chord z-positions are shown in Fig. 4.

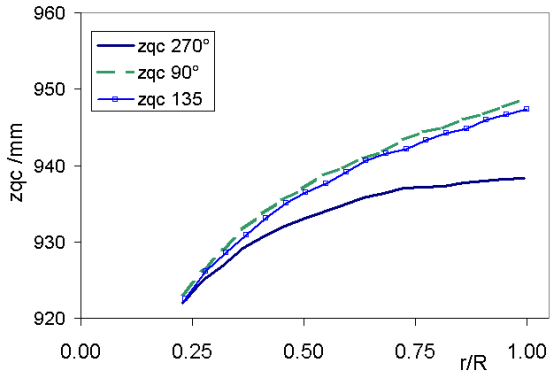

Fig. 4 Quarter chord line z-position of Ψ=90°, Ψ=135° and Ψ=270° in wind tunnel coordinate system after rotation by the shaft angle (non-rotating)

These results indicate an existing roll angle. The correct roll angle was identified by adapting the z-coordinates of the quarter chord line of Ψ=90° and Ψ=270° to get a constant offset between them. For these calibration data the roll angle was investigated manually to Φ=0.175°. Now the offset in z-direction is only about 2 mm compared to 7 mm by using the old raw data. This reduction is a result of the new calibration.

To note is that a roll angle of Φ=0.175° means a tip deflection in z-direction of about Δz_{tip}=6 mm for each side, thus about 12 mm difference between advancing and retreating side, which is far above the measurement accuracy.

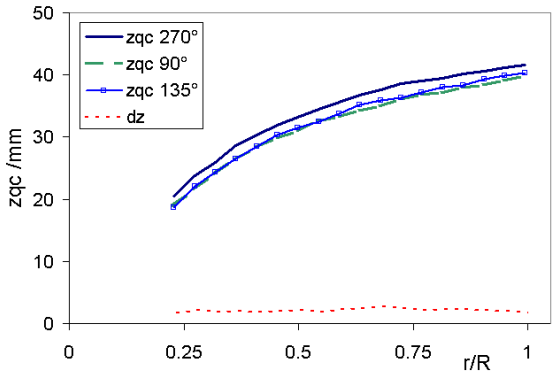

Fig. 5 Quarter chord line z-position of Ψ=90°, Ψ=135° and Ψ=270° in rotor hub coordinate system after rotation by the shaft and roll angle (non-rotating)

Analyzing methods

Averaging

One data point is composed of mostly 50, some times 100 images. To get smooth data with reduced errors and eliminated vibrations it is necessary to determine averages of the coordinates. To average the marker coordinates a mean value for each marker of all repeats (if there were no errors) was computed. As described in [1] the scattering has a range of 2.6 mm in z-direction (positive up), of about 1.1 mm in x-direction (wt-system: positive downstream). The maximum deviations found were in y-direction (wt-system: positive right) of about 4.7 mm because of the minor stiffness of the wind tunnel sting in this direction and associated vibrations in a wide frequency range. In general the scattering of the blade markers depends on the distance to the rotor hub and the blade azimuth. With increasing radius the scatter is growing because of the blade elasticity (blade flapping, lead lag and torsion motion) in addition to the body vibrations and the sting motion.

Drift compensation

As described in [1] marker position displacements due to low frequency motions of the wind tunnel sting and vibrations of the rotor model and support were present during the measurements. Based on the drift of the body markers all blade marker coordinates were modified and the results by using the old raw data have shown that the body marker positions differ in measurements of the advancing and retreating side. The difference between the mean value of one azimuth to the mean value from all azimuths define the body drift.

On analyzing the "old" raw data in view of the body motion and drift compensation it was necessary to separate into mean values of the advancing and retreating side, since the measured body marker coordinates have an offset in each direction. That's why the drift compensation was separated and independently applied to advancing and retreating side. By using the "new" calibration method (10 calibration markers plus 2 body marker locations) there is only a very small offset remaining and thus no separation in adv. and ret. side is necessary. Furthermore the coordinates at Ψ=180° are usable.

In Fig. 6 the z-position of body marker #3 is shown. In general there is a drift in positive z-direction. By using the "old" raw data calibrated by 6 calibration markers an offset is present between advancing and retreating side and the coordinate at Ψ=180° is unreliable.

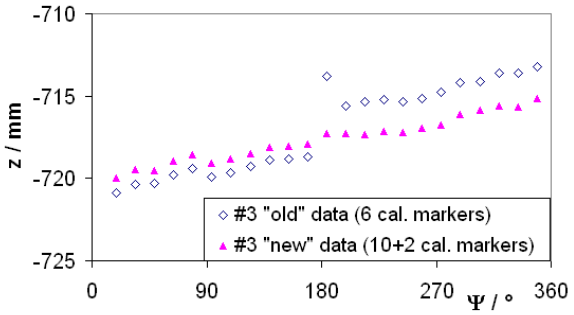

Fig. 6 Effect of new calibration of coordinates of body marker #3 in z-direction (wind tunnel system) for case BL5.3

A comparison of the deviations of both by using the old and the new raw data show an improvement of the results especially at Ψ=180°. The skip of about 4.5 mm is reduced of less than 1 mm in x- and z-direction and thus within the measurement accuracy. This leads to the conclusion that a separation into advancing and retreating side is not necessary by using the new raw data.

Further investigations have shown that an elimination of the sting movement is not necessary any longer because due to the determination of the rotor hub center by circular regression there is only a deviation in y-direction which is eliminated by shifting into the hub center. The results in lead-lag-motion are the same with or without a correction of this sting move.

The new raw data which contain the data of all four blades have shown that this sting movement

was also present in other configurations. In MN5.3 (compare Fig. 7) and in the case BL3.7 it happened just before 15° azimuth of the reference blade. That is why it was not visible in the old raw data. However, it can be seen in the data of the other three blades. This is a proof that it is necessary to measure all blades in order to identify effects like these.

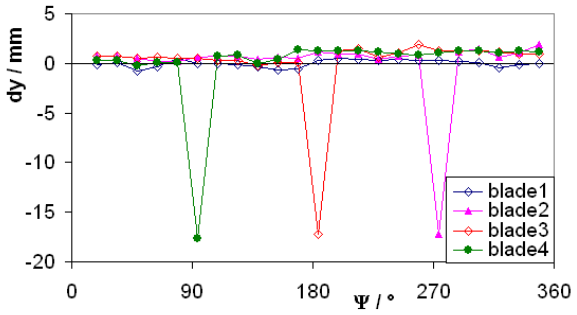

Fig. 7 Body marker drift in y-direction, all four blades (MN5.3)

Due to the drift correction and the shifting of all marker coordinates the sting movement has no influence on the blade motion analyzed with respect to the rotor hub center position. After determination of the body marker drift the blade marker positions can be corrected by this drift.

Rotation

To obtain the parameters of blade motion, the data in DNW coordinate system have to be transformed into the rotor hub coordinate system. This is done by rotating the coordinates by the rotor shaft angle and the rotor roll angle in a coordinate system parallel to the rotor shaft and transformation (shifting) of all marker coordinates into the rotor hub location. Previously the raw data were prepared without taking into account a roll angle.

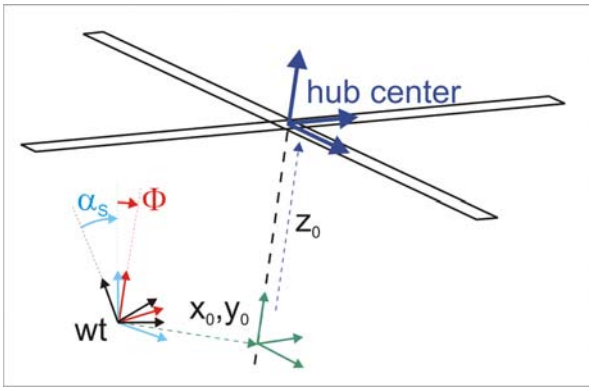

Fig. 8 Transformation procedures from wind tunnel into rotor hub coordinate system

The investigations have demonstrated that a roll angle was present during all measurements. That is why this roll angle has to be considered in the coordinate transformation. After transforming all coordinates in the rotor hub system (see Fig. 8) the parameters of flap, lead lag and torsion motion of the rotor blades can be calculated.

Rotor hub center

Three different calculation methods for determining the rotor hub position were evaluated [1] and the advantages and drawbacks of each method were described to find out the best qualified results.

The best method for center point determination was identified to be the circular regression (compute best fit circles of the positions of one single blade marker, Fig. 9) over all azimuths.

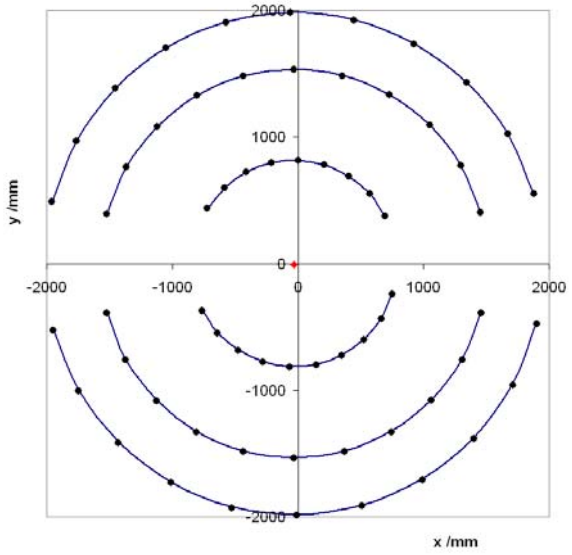

Fig. 9 Exemplary best fit circles for r/R = 0.4, 0.77, 1 (BL5.3)

Fig. 10 shows a comparison of the hub center coordinates by using the old and the new raw data exemplary for the minimum vibration configuration. The calculation with the new data leads to a shifted hub center position in x-direction of about +2.5 mm. In the other configurations this shift is similar between 1.5 to 2.5 mm. The scatter in y-direction is becoming smaller from 4 mm by using the old data to 2.5 mm now.

In all configurations a small drift in negative y-direction is identifiable with respect to increased blade marker radius. The hub center point coordinates by calculation with all azimuths have no remarkable drift in x-direction (less than 0.5 mm). There is only a small difference (0.3 mm) be-

tween the computed center points of front and rear blade marker, well within the measurement accuracy.

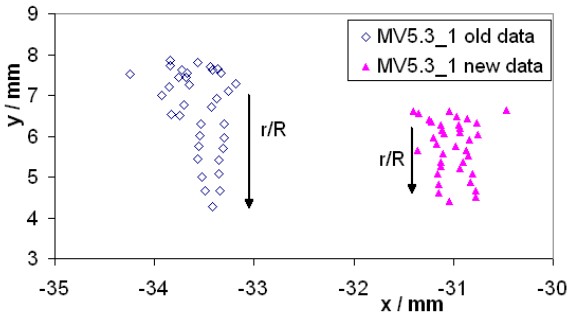

Fig. 10 Comparison of rotor hub center position (MV5.3 blade #1, old and new data)

Beside the comparison between old and new data now we can compare the calculated rotor hub center positions by using the four blades. An example result is shown in Fig. 11 for all four blades of the minimum vibration case. Only the inner 10 blade markers were used.

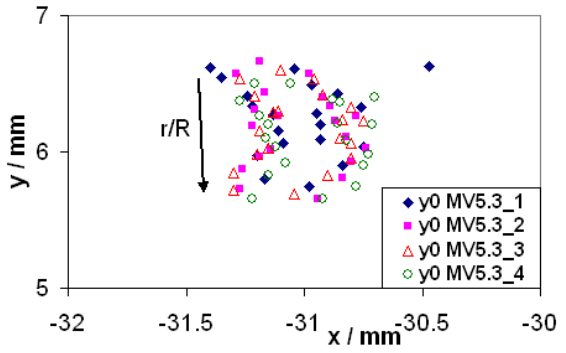

Fig. 11 Comparison of rotor hub center position (MV5.3 blade #1 to #4, new data)

With regard to scattering there is a maximum of about 1.0 mm in x-direction and 1.1 mm in y-direction in all configurations. Comparing the scatter of the new data with the scatter by using the old data (maximum x: 1.6 mm, y: 4.5 mm) the newer data lead to much less scatter and thus it can be assumed that they are more accurate, especially when only the inner radii blade markers are used. They are not subject to significant flapping deflections and thus on more perfect circles than the outer markers.

When the hub center positions of the different blades are compared, the maximum blade-to-blade deviation is about 0.8 mm in x-direction and only 0.2 mm in y-direction. In conclusion the new raw data are more accurate and the blade-to-blade differences are in the order of the SPR measurement accuracy.

After the hub center coordinates in x- and y-direction are found, the position in z-direction of the rotor hub center is in demand. At first the coordinate system must be shifted into the hub center found so far. This means a transformation of all blade and body markers into a coordinate system with the origin in the rotor hub x-,y-center point, while the origin in z is yet anywhere on the shaft axis (see Fig. 8).

To identify the rotor hub z-coordinate, a polynomial of fourth order with an additionally constraint is used. It is assumed that the gradient dz/dr at the position where the blade is fixed is equal to the precone angle of 2.5° as a boundary condition (see Fig. 12). The least error squares method is used again to obtain the remaining coefficients of the polynomial function. More information about this method can be found in [1].

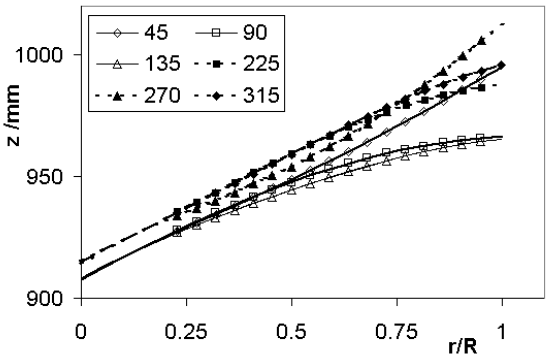

Fig. 12 Best fit polynomials for different azimuths for MN5.3

By using the old raw data there was a vertical offset of about 7 mm in each configuration between advancing and retreating side. This was mainly caused by the calibration. As mentioned above the newer data in non rotating system leads to a remaining offset of about 2 mm after the transformations in the non-rotating system. The calculation of the hub center coordinates in z-direction results in significantly smaller offsets between advancing and retreating side. Fig. 13 shows the comparison of the z_0 coordinates of the old and new data, exemplary for the reference blade of the minimum noise configuration.

Caused by the improved raw data and the transformation with respect to the model roll angle the offset has decreased to about 2.4 mm. This offset range can be found in the other configura-

tions as well. Further it can be noticed that the blade-to-blade differences with an average of about 0.8 mm are very small (e.g. in Fig. 14). Since all blades exhibit this offset between advancing and retreating side this is a systematic measurement error of yet unknown nature.

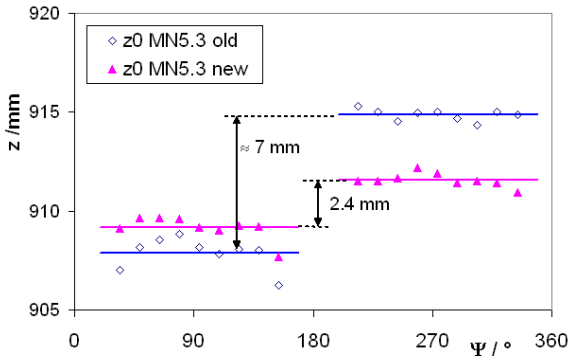

Fig. 13 Comparison of rotor hub center position in z-direction for old and new data (MN5.3 blade #1)

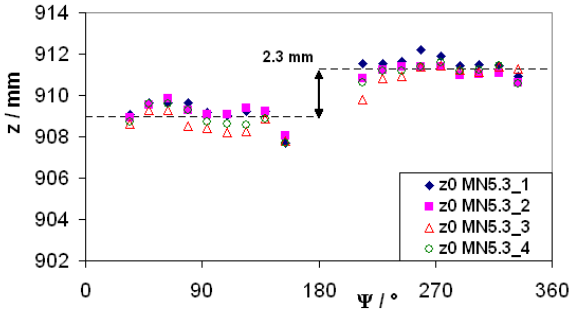

Fig. 14 Rotor hub center z-coordinate (MN5.3 all blades)

With the z-position of the rotor hub the coordinate system can be shifted into the final rotor hub coordinate system. Because of the offset the shifting is done separated with respect to advancing and retreating side.

Results

Blade lead-lag motion

With respect to the elastic blade lead-lag displacement (lag positive) there was an unexplained behavior in the time history of the cases BL5.3 and BL11.5 as found in [1]. In the first quarter of Fig. 15 this problem is visible for BL5.3. In further investigations it was found that this problem is not mainly caused by the sting movement in y-direction.

The wind tunnel sting has two hinges with vertical axis. Thus it is possible to give the model a yaw angle (called beta). The angle of each hinge can be measured and the sum of both leads to the model yaw angle beta. For the HART II tests this yaw angle should have been zero, but caused by unknown reasons it has had a range between 0.24° and -0.02° (positive in rotation direction). This results in an apparent lag deflection of about 8 mm at the blade tip (see Fig. 15).

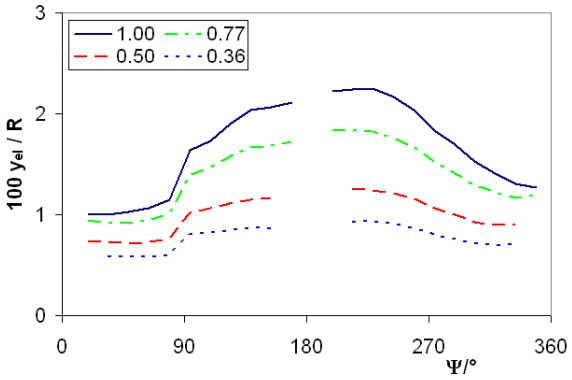

Fig. 15 Blade lead-lag motion for different radii (BL5.3 old data, blade #1)

To correct the model yaw angle in calculations the associated beta angle has to be added to the blade azimuth. There are measured data of the beta angle for each azimuth available. Thus the elastic blade lead-lag is given by the distance between the radial position of the quarter chord line and a straight line defined by the current azimuth position of the blade plus the yaw angle beta. In Fig. 16 an example of the model yaw angle beta for the reference blade of the case BL5.3 is shown. It is clearly visible that there are greater yaw angles in between 15° and 75°, which is the range where the skip in the lag motion is, visible in Fig. 15.

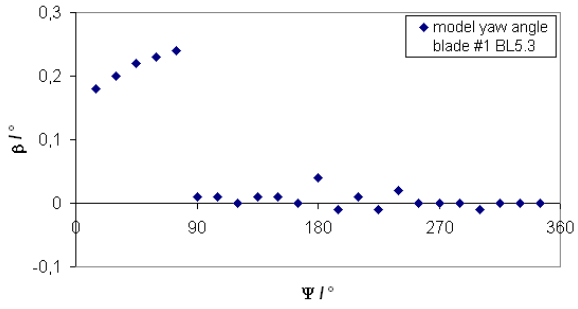

Fig. 16 Model yaw angle β (BL5.3 blade #1)

When the yaw angle correction is applied to the lead-lag calculation the skips in the time history can be eliminated. Compared to the results in

Fig. 15 the skip between 75° and 90° is eliminated. The tip deflection for the case BL5.3 is shown in Fig. 17.

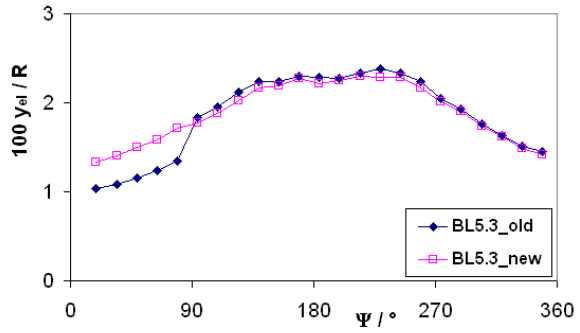

Fig. 17 Comparison of blade tip lag motion (BL5.3 old and new data, blade #1)

The comparison of the concerned azimuth positions with the data for the model yaw angle leads to the result that even at these azimuth positions a higher yaw angle was present. Thus all calculations were made by using the yaw angle correction which leads to non-constant azimuth steps (15° ± 0.2°).

The blade-to-blade comparison of the tip deflection time history leads to a maximum difference of about 9 mm in the BL11.5 configuration and to a minimum difference of about 0.9 mm in the MN5.3 configuration (Fig. 18).

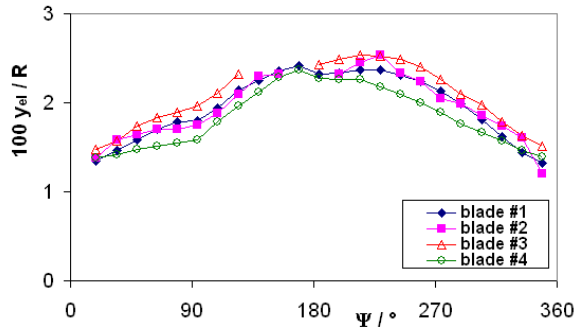

Fig. 18 Elastic blade tip lead-lag motion (MN5.3)

The radial distributions of the elastic blade lag position are shown in Fig. 19 exemplarily for the case MN5.3. The results were chosen at an azimuth of Ψ=229°. There is nearly a linear dependence of the lag value with respect to the radius in each configuration. Conspicuous is the curve at inner radii.

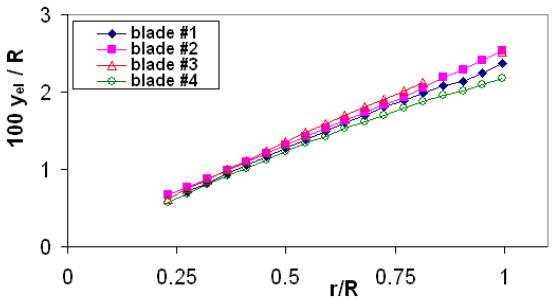

Fig. 19 Radial distribution of blade lag motion at Ψ= 229° (MN5.3)

For a hingeless rotor as used here they should have a value and a gradient of zero at the position of the blade fixation at r/R=0.1. But in all configurations at all azimuths this is not the case. An extrapolation to radius r/R=0.1 with an additional constraint (gradient $dy_{el}/dr=0$) leads to an offset of about 10 mm. Fig. 20 shows the radial distribution of blade lag position for the reference blade of BL5.3 with measured and polynomial values, using this constraint.

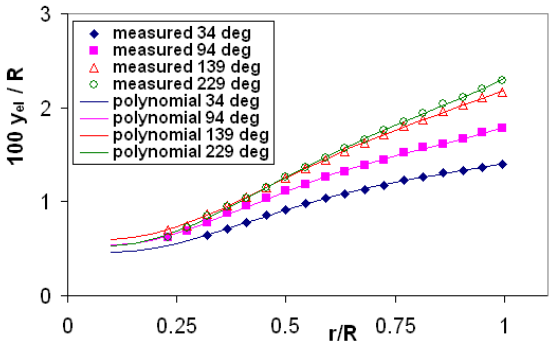

Fig. 20 Radial distribution of blade lag motion, measured and polynomial (BL5.3 blade #1)

Since this problem can be found in all configurations and azimuths it is a systematic error. In principle this offset indicates a distance of the quarter chord line to the rotor hub center. For a better understanding Fig. 21 shows the quarter chord lines extrapolated to the rotor hub center. The position where the blades are fixed is at r/R=0.1 (200 mm).

Another reason could be a gradient dy_{el}/dr unequal zero which means a build-in angle at the blade fixation. But since the problem is identifiable at all four blades and the value of the offset is sizable this reason is not realistic. Up to now there is no explanation for this.

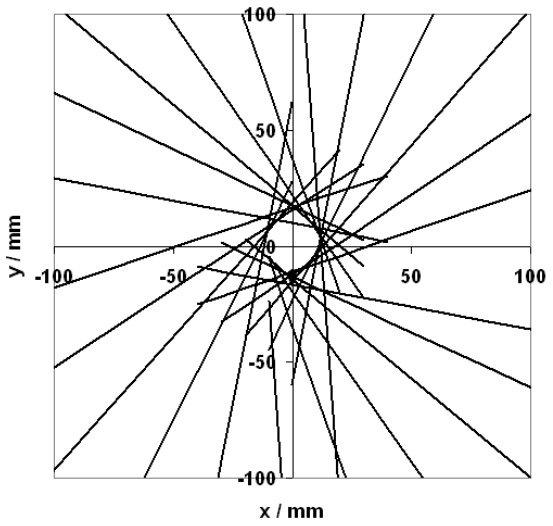

Fig. 21 Extrapolated quarter chord lines (BL5.3 blade #1)

Blade Flap motion

The elastic blade flap deflection z_{el} (positive up) is given by the distance between the quarter chord line and a straight line defined by the pre-cone angle. Therefore approximately the distance of the quarter chord line z-position to the pre-cone line at defined radial positions is used. Compared to the results of the old raw data a modified curve of the elastic blade flap time history is obtained, due to the correction of the raw data by the model roll angle and the new calibration. Because of the direction of the roll angle the correction leads to lower elastic blade flap values at the advancing side and higher values at the retreating side. Fig. 22 shows the elastic blade tip deflection in z-direction in the rotor hub coordinate system for the reference blade of the case BL5.3 compared with the same results by using the old raw data and no roll angle correction.

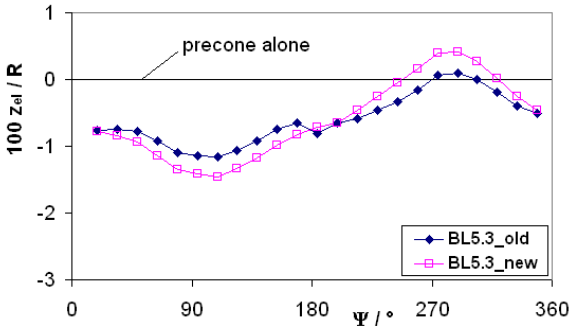

Fig. 22 Comparison of elastic blade tip flap motion (BL5.3 blade #1, old and new data)

It clearly can be seen that the roll angle correction has a substantial influence to the elastic blade deflection. Furthermore the skip between advancing and retreating side at Ψ=180° is eliminated and the value at Ψ=180° is usable.

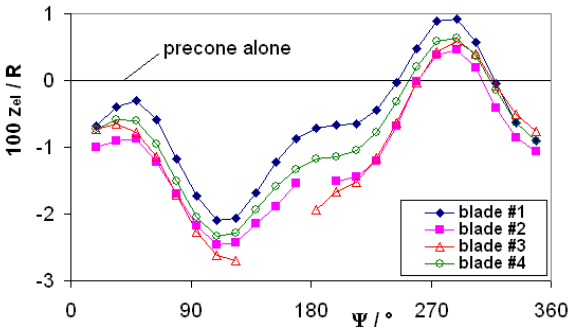

Fig. 23 Elastic blade tip flap motion (MN5.3)

The maximum blade-to-blade difference is about 20 mm mainly in the vicinity of Ψ=180°. The greatest values can be found for the reference blade #1 followed by blade #4 and #2. In all configurations blade #3 has the smallest values (see Fig. 23). Reason could be an incorrect blade tracking at the beginning of the wind tunnel tests or different blade elasto-mechanical properties. The same tendency is visible in the radial distributions of all four blades. In Fig. 24 the results for MN5.3 at an azimuth of Ψ=90° are shown.

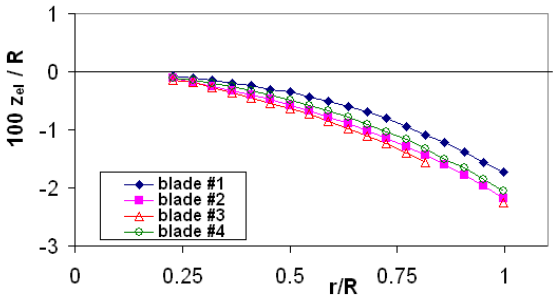

Fig. 24 Radial distribution of elastic blade flap (MN5.3)

BTD results

In addition to the SPR measurements the common support was used for one camera focusing on the 90° azimuth position of the blade, and a second tower was holding another camera for a view on the 135° position. These two cameras were focused only on the blade tip at the respective azimuth positions and measured the deflections of the blade tip. The setup is schematically given in Fig. 1. Measured were the coordinates of the leading and trailing edge. To compare the

SPR and BTD results the coordinates of the leading and trailing edge were transformed into the blade marker positions.

The following figures (Ψ=90° in Fig. 25, Ψ=135° in Fig. 26) compare the z-coordinates in the wind tunnel system. The BTD results are plotted exemplarily for the minimum noise configuration together with the SPR raw data. At Ψ=90° the differences between SPR and BTD data have a range from 0.2 mm (blade #4 front) to -6.0 mm (blade #3 rear). The maximum blade-to-blade difference by using BTD is about 10 mm between blade #1 and #2 at the rear marker position.

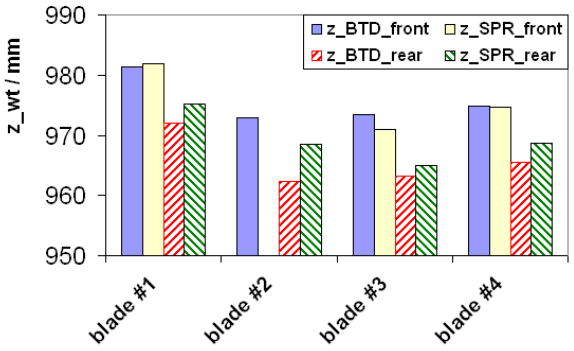

Fig. 25 Comparison of BTD and SPR data in z-direction at Ψ=90° (MN5.3)

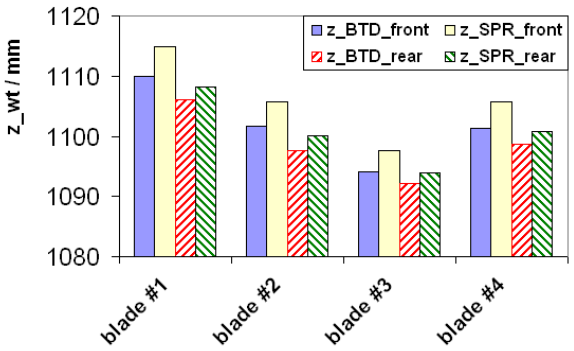

Fig. 26 Comparison of BTD and SPR data in z-direction at Ψ=135° (MN5.3)

At a blade azimuth of Ψ=135° (Fig. 26) there is a maximum blade-to-blade difference by using BTD of about 16 mm between blade #1 and #3. The differences between SPR and BTD data have a range from -1.8 mm (blade #3 rear) to -4.8 mm (blade#1 front). In general the tendency that blade #1 has the greatest z-values and blade #3 the smallest is confirmed.

Blade torsion motion

As described in [1] the pure elastic pitch deformation (ϑ_{el} positive nose up) can be calculated by the distance of the z-coordinate of the front and rear blade marker, the associated pitch control angle, the pretwist angle and the pitch offset in z-direction due to the different distance of the front and rear blade markers to the quarter chord line. The view on the comparison between the results by using the old and new raw data leads to no major differences (compare Fig. 27). There is a maximum deviation of about 0.3°at Ψ=169°. In principle by using the new raw data a smoother curve can be obtained especially near the azimuth position of Ψ=180°.

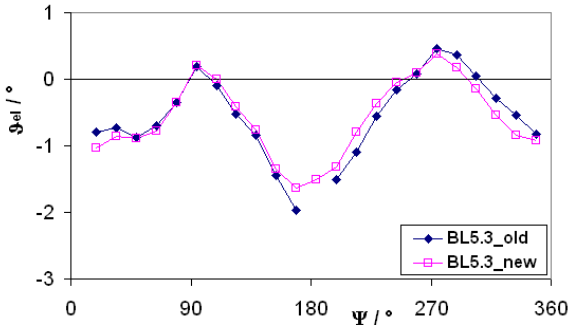

Fig. 27 Comparison of blade torsion motion (BL5.3 blade #1, old and new data)

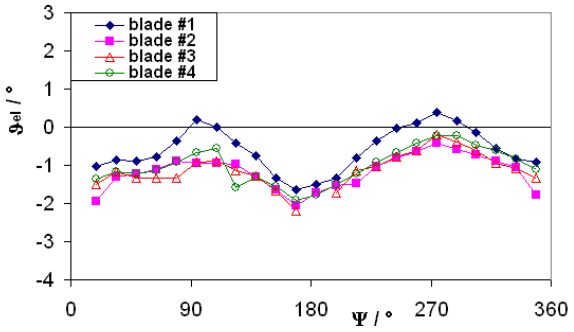

Fig. 28 Time history of the elastic blade torsion (BL5.3 all blades)

The blade-to-blade differences have a range of about 0.1° to 1.4° (minimum vibration Ψ=94°). In general blade #1 has the greatest torsion values, the values of blade #3 are the smallest (compare Fig. 28). Fig. 29 shows the radial distributions of the elastic blade pitch at an azimuth position of Ψ=139° for the BL5.3 configuration. The maximum scatter found for a neighboring blade marker pair is about 0.8°.

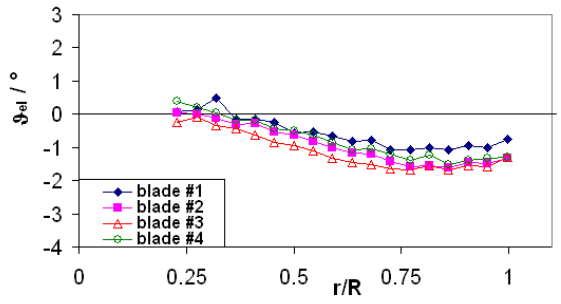

Fig. 29 Radial distribution of elastic torsion (BL5.3 all blades, Ψ=139°)

An assumed accuracy of marker position recognition of 0.4 mm and the distance between front and rear marker centers of 89 mm leads to a theoretical error of:

$$error = \arctan\left(\frac{2 \cdot 0.4mm}{89mm}\right) \approx 0.52°$$

Thus the computed torsion values have a maximum scatter which is out of the range of the assumed measurement error. Furthermore at some azimuth positions the calculated blade pitch distribution has computed torsion values which are definitely outside of the expected curve (example in Fig. 30 grey range). Investigations have shown that reflections on the blade near the leading edge at azimuths near Ψ=90° and Ψ=270° have falsified the marker position recognition. This problem is found in all measurement configurations. The reflections are at the leading edge and they come from the stroboscopic flashes. Due to these reflections the usual black background is more brightly and the contrast to the white markers is small. The recognition of a correct marker bound is difficult and the recognized marker centers have incorrect coordinates, leading to error in the torsion.

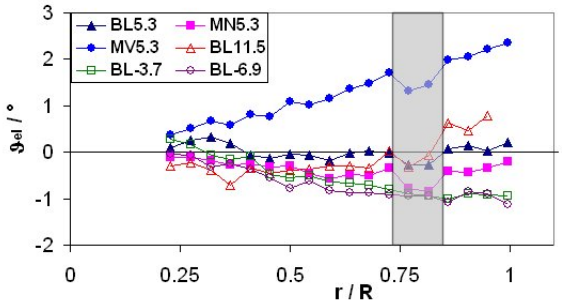

Fig. 30 Radial distribution of elastic torsion at Ψ=90° (all configurations)

A possibility to get better results would be to compute a regression function. To reduce measurement noise and smooth out irregularities, polynomial functions of fourth order were carefully fitted through the positions of the leading and trailing edge markers and differentiated to get the local pitch. The results by using this method were unacceptable at inner radii [1]. That is why a second approach was applied. The basis for the regression function is the first mode shape of blade torsion $\Phi_1(r^*)$. The second torsion mode shape has not to be considered since the according natural frequency is at about 10/rev. By using the least error squares method the coefficients ϑ_0 and ϑ_1 were computed.

$$\vartheta_{el}(r) = \vartheta_0 + \vartheta_1 \cdot \Phi_1(r^*)$$

$$r^* = \frac{r - r_E}{R - r_E}$$

r_E is the radius at the blade main bolt and Φ_1 the first mode shape of torsion (coefficients by FEM).

$$\Phi_1(r^*) = \sum_{j=0}^{J} c_j \cdot r^{*j}$$

An example for different azimuths is shown in Fig. 31 for the reference blade of the minimum noise configuration. By using the mode shape representation results are smooth curves with a value unequal zero at the blade fixation r/R=0.1. In the example figure the radial distribution at an azimuth of Ψ=244° has an elastic torsion value of 0.55° at this position.

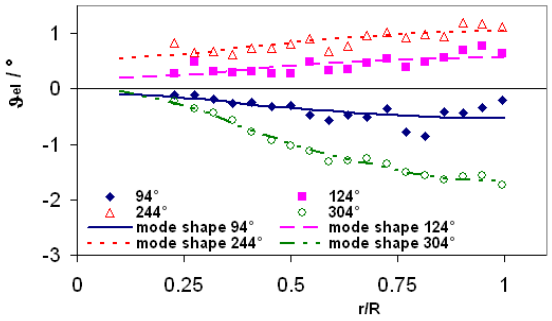

Fig. 31 Elastic blade torsion, measurements and mode shape regression (MN5.3)

In general the elastic torsion values at inner radii lead to the conclusion that there is a systematic error because most of the radial distributions have values in the vicinity of about ϑ_{el}=0.5° at the blade fixation (compare Fig. 32). The root offset can have several reasons. The blade tracking was done by setting different root pitch offsets. A

steady offset could also by caused by the used pitch data which come from the acoustic part of the test. During the SPR measurements there was a sensor defect. A possibility for a dynamic offset is the increasing loose of the pitch bearings in the course of the tests.

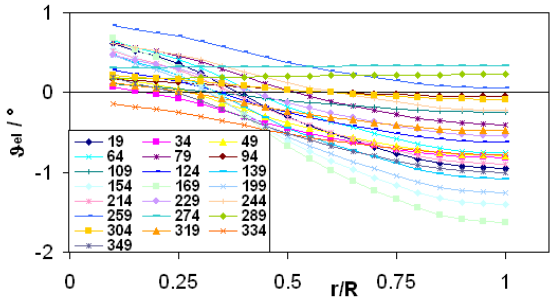

Fig. 32 Elastic blade torsion mode shape regression (BL5.3)

The comparison of the time history of the blade torsion yields no major difference between the measured elastic torsion angle and the mode shape based regression function. The results of the elastic torsion angle from data in the non-rotating system have shown that the scatter at each three azimuth positions is about ±0.5°. The maximum deviation of about 1.0° could be found at Ψ=90°.

In conclusion the results obtained for blade torsion depend on several conditions. There is the theoretical error by marker position recognition of about 0.5°, possible offsets due to the blade tracking and the accuracy of all 4 blades root pitch angle measurements. Further the calculation of the torsion angle by differentiation leads to increased errors. Thus to obtain better results for blade torsion a simultaneous measurement of the blade root pitch angle and SPR is necessary.

Alpha sweep

In the following figures the elastic flap (Fig. 33), lead-lag (Fig. 34) and torsion (Fig. 35) motion of the reference rotor blade (blade #1) depending on azimuth are shown. There is a comparison of the α-sweep configurations at the blade position at r/R = 99%.

In flapping and torsion a 2/rev motion is present in descent. In the lead-lag motion there are nearly constant amplitudes of about 10 mm in 1/rev at the blade tip. By using the new raw data and the model yaw angle correction the skips in the cases BL5.3 and BL11.5 are eliminated. The maximum lag value increases from descent to climb as expected by the increased power consumption. In the time history of the elastic torsion the 2/rev oscillation is stronger in descent than in climb condition.

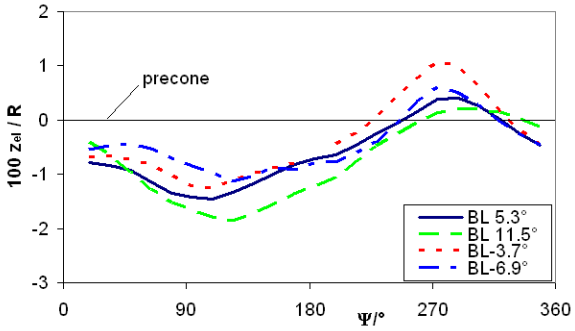

Fig. 33 Blade tip flap motion depending on azimuth for α-sweep (r/R = 99%, blade #1)

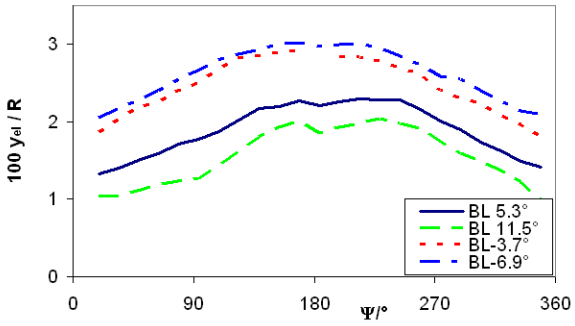

Fig. 34 Blade tip lead-lag motion depending on azimuth for α-sweep (r/R = 99%, blade #1)

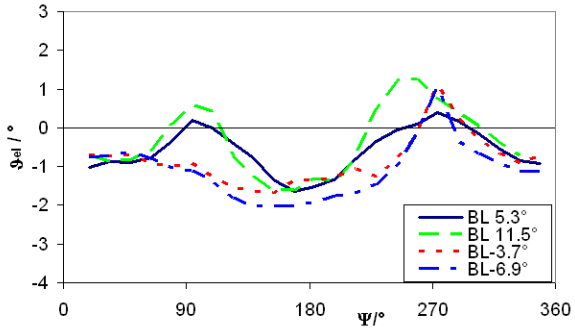

Fig. 35 Elastic torsion motion depending on azimuth for α-sweep (r/R = 99%, blade #1)

HHC sweep

The following figures show the comparison of the elastic flap (Fig. 36), lead-lag (Fig. 37) and torsion (Fig. 38) motion of the rotor blade depending on azimuth for the configurations with higher harmonic control and the base line case at the blade position r/R=99%.

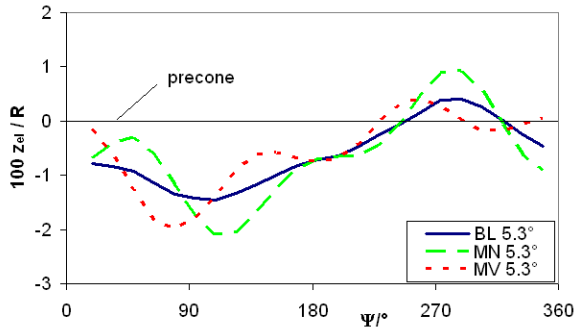

Fig. 36 Blade tip flap motion depending on azimuth for HHC sweep (r/R = 99%)

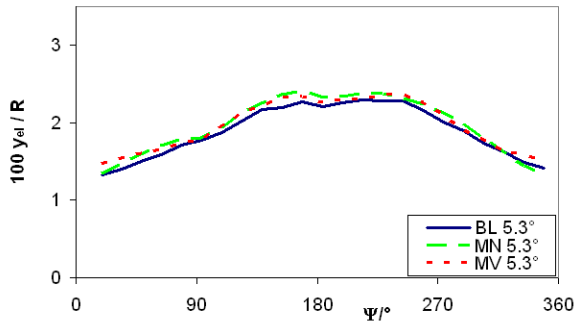

Fig. 37 Blade tip lead-lag motion depending on azimuth for HHC sweep (r/R = 99%)

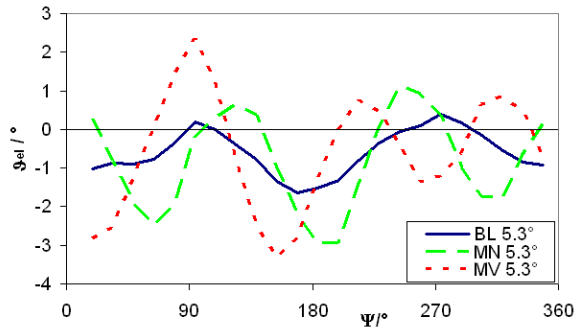

Fig. 38 Elastic torsion motion depending on azimuth for HHC sweep (r/R = 99%)

When 3/rev HHC is applied (cases MN and MV), a 3/rev flapping dominates the figure (Fig. 36) as expected. The local amplitudes are up to 12 mm off the BL position at the blade tip in the minimum noise case. The results of the blade lag motion show nearly identical values with 1/rev amplitudes of about 10 mm independent of the higher harmonic control.

With 3/rev HHC a strong 3/rev torsion is the response which was expected due to the natural frequency in torsion at 3.6/rev of this rotor. The local amplitudes in torsion are up to 1.5° off the BL position in the minimum noise case and up to 2.5° in the minimum vibration case.

Conclusions

1. The new calibration method leads to significantly improved accuracy of the raw data.

2. By using the data of all four blades several problems could be solved.

3. The accuracy of SPR is confirmed.

4. For blade torsion a simultaneous measurement of the blade root pitch angle and SPR is necessary because of the dependence of the results on the accuracy of blade root pitch measurement and the blade tracking.

5. A remaining open question is the blade lead-lag root offset.

Recommendation: SPR measurements from the rotor hub center in the rotating system could eliminate lots of problems.

Acknowledgement

An international test as complex as HART II requires a lot of engagement of all participants, both in the fore- and in the background. It would fill pages to name everybody. Instead, the teams are specifically addressed. These are: the prediction team, the test team and the management team, all of them consisting of US/French/German members working years ahead in real partnership preparing the rotor hardware, the measurement techniques, the test matrix and the funding. Specifically the funding of the test from US and French side, the development of 3C-PIV and preparation of the rotor and conduction of the test on DLR side shall be mentioned, and the strong support of DNW during the test. Without the enthusiasm of all of them this test would never have come true - thanks to all of them!

References

[1] **Meeting Paper –** O. Schneider, B.G. van der Wall, K. Pengel, *HART-II Blade Motion Measured by Stereo Pattern Recognition (SPR)* -, 59th Annual Forum of the American Helicopter Society, Phoenix, USA, 2003

[2] **Meeting Paper -** Yu, Tung, van der Wall, Pausder, Burley, Brooks, Beaumier, Delrieux, Mercker, Pengel, *The HART-II Test: Rotor Wakes and Aeroacoustics with Higher-Harmonic Pitch Control (HHC) Inputs - The Joint German/French/Dutch/US Project* -, 58th Annual Forum of the American Helicopter Society, Montreal, Canada, 2002

[3] **Meeting Paper -** B.G. van der Wall, B. Junker, C.L. Burley, T.F. Brooks, Y.H. Yu, C. Tung, H. Richard, M. Raffel, W. Wagner, K. Pengel, E. Mercker, P. Beaumier, Y. Delrieux, *The HART II Test in the DNW – a Major Step towards Rotor Wake Understanding*, 28th European Rotorcraft Forum, Bristol, UK, 2002

[4] **Meeting Paper -** K. Pengel, R. Müller, B.G. van der Wall, *Stereo Pattern Recognition – the Technique for Reliable Rotor Blade Deformation and Twist Measurement*, AHS International Meeting on Advanced Rotorcraft Technology and Life Saving Activities, Utsunomiya, Tochigi, Japan, 2002

[5] **Meeting Paper** - B. Gelhaar, B. Junker, W. Wagner, DLR – *Rotor Teststand Measures Unsteady Rotor Aerodynamic Data*, 19th European Rotorcraft Forum, Cernobbio, Italy, 1993